

Fast and Slow Inactivation of Sodium Channels: Effects of Photodynamic Modification by Methylene Blue

J. G. Starkus, M. D. Rayner, A. Fleig, and P. C. Ruben

Bekey Laboratory of Neurobiology and Department of Physiology, John A. Burns School of Medicine, University of Hawaii, Honolulu, Hawaii 96822 USA

ABSTRACT Illumination of crayfish giant axons, during internal perfusion with 0.5 mM methylene blue (MB), produces photodynamic effects that include (i) reduction in total sodium conductance, (ii) shifting of the steady-state inactivation curve to the right along the voltage axis, (iii) reduction in the effective valence of steady-state inactivation and, (iv) potentially complete removal of fast inactivation. Additionally, the two kinetic components of fast inactivation in crayfish axons are differentially affected by MB + light. The intercept of the faster component (τ_{h1}) is selectively reduced at shorter MB + light exposure times. Neither τ_{h1} nor the slower (τ_{h2}) process was protected from MB + light by prior steady-state inactivation of sodium channels. However, carotenoids provide differing degrees of protection against each of the photodynamic actions listed above, suggesting that the four major effects of MB + light are mediated by changes occurring within different regions of the sodium channel molecule.

INTRODUCTION

Voltage-clamp studies of thiazine dyes (Pooler, 1968; Pooler, 1972; Pooler and Oxford, 1973; Oxford et al., 1977) have documented photodynamic damage following both extracellular and intracellular application of these agents. Effects reported included an irreversible reduction in peak sodium and potassium conductance; an increase in time to peak I_{Na} ; and slowing of the time constant for fast inactivation with right shifting of the steady-state inactivation curve in lobster axons (Pooler, 1972) but not in squid axons (Oxford et al., 1977). By contrast, Croop and Armstrong (1979) reported that, in the absence of light, intracellular application of thiazine dyes produces a fully reversible block of sodium conductance. Previous work with these agents had not clearly distinguished between this reversible channel block and the irreversible photodynamic effects.

Subsequent studies of channel block by thiazine dyes (Armstrong and Croop, 1982; Starkus et al., 1984) have been carried out under low ambient illumination. Under these conditions thiazine dyes have been described as "inactivation simulators," since they "inactivate" sodium channels (after the removal of fast inactivation by pretreatment with pronase) both with a time course similar to that of normal inactivation and with simultaneous immobilization of the gating charges (Armstrong and Croop, 1982). Time-dependent block of sodium conductance results from binding to a site accessible from the cytoplasmic side of the membrane. The binding is fully reversible, occurs only in "open" sodium channels, and appears to compete with the normal fast inactivation mechanism. There is no accumulation of block at interpulse intervals greater than a few milliseconds, and full

return to control kinetics occurs following washout of the dye (Starkus et al., 1984).

The full reversibility of block by thiazine dyes suggested their use for checking internal perfusion rate during axial-wire voltage clamp experiments. We have found that the intense color produced by the addition of 0.5 mM methylene blue (MB) permits the internal perfusate to be readily visualized within crayfish giant axons even under minimal illumination. However, after one such perfusion test, during which our transillumination light source was accidentally left on, we noticed an irreversible removal of fast inactivation after washing out the MB solution. This observation reawakened our interest in photodynamic effects and prompted the present study. For internally perfused giant axons, the duration of illumination can be more precisely controlled than the duration of exposure to inactivation-modifying agents. By controlling illumination duration in the presence of a "maximal" MB concentration, we show that the two kinetic components of fast inactivation (τ_{h1} and τ_{h2}) are differentially affected by MB + light. Additionally, controlled photodynamic effects support the hypothesis of Ruben et al. (1992), that the right shift of the steady-state inactivation curve is a separate direct effect of inactivation-modifying agents rather than an indirect result of fast inactivation removal. Finally, we have explored protection by carotenoids against the photodynamic effects of MB (see Oxford et al., 1977). We find differing levels of protection against sodium channel loss, fast inactivation removal, and the right shifting of steady-state inactivation, suggesting that these effects are mediated by damage to different regions of the sodium channel molecule.

Preliminary reports of this work have been presented (Fleig et al., 1992; Starkus et al., 1993a).

Received for publication 11 November 1992 and in final form 29 April 1993.

Address reprint requests to Dr. John G. Starkus, Bekey Laboratory of Neurobiology, 1993 East-West Road, University of Hawaii, Honolulu, HI 96822.

© 1993 by the Biophysical Society

0006-3495/93/08/715/12 \$2.00

MATERIALS AND METHODS

Crayfish medial giant axons were dissected free, internally perfused, and voltage-clamped following methods initiated by Shrager (1974) and modified by Starkus et al. (1984). Axons were maintained between 6°C and 8°C

with a feedback-controlled Peltier device; potassium currents were blocked by internal perfusion with solutions containing Cs ions. Pulse generation, data recording techniques, methods for continuous adjustment of series resistance compensation, subtraction of linear capacity, and leakage currents were as described by Rayner and Starkus (1989), Alicata et al. (1989), and Starkus and Rayner (1991). All experiments were carried out using reduced Na solutions so as to maintain a peak ionic current no greater than ~ 1 mA/cm² under control conditions. Internal perfusates contained (in mM): 0 Na, 0 K, 230 Cs, 60 F, 170 glutamate, 1 4-(2-hydroxyethyl)-1-piperazineethanesulfonic acid (adjusted to pH 7.35), to which methylene blue (Aldrich Chemical Co., Milwaukee, WI) was added at 0.5 mM, when required, without other adjustments. External perfusates typically contained (in mM): 50 Na, 13.5 Ca, 2.6 Mg, 160 TMA, 242.2 Cl, and 2 4-(2-hydroxyethyl)-1-piperazineethanesulfonic acid (adjusted to pH 7.55). Any further adjustments of external sodium were achieved by substitution of tetramethylammonium (TMA) for sodium ions. Preliminary experiments, using carotenoid compounds as potential antagonists of methylene blue photoexcitation, showed similar effects with β -carotene (Sigma Chemical Co., St. Louis, MO), lycopene, and canthaxanthin (Hoffmann-LaRoche, Basel, Switzerland). All results reported here were obtained by adding sufficient carotenoid to the internal perfusate to give a 10 mM final concentration, using tetrahydrofuran as an initial solvent (0.5% final concentration) to counter the very low solubility of carotenoid agents in aqueous solutions. No effects of tetrahydrofuran on the conductance or kinetics of sodium channels were found at this concentration in control experiments. However, some of the carotenoid precipitated during perfusion, and final concentrations within the axon were lower than 10 mM.

Final dissection of the selected medial giant axon from the nerve cord was carried out in the experimental chamber. This chamber has a lucite bottom to permit transillumination of the axon, which is visualized with a Wild M5A stereo microscope. Illumination was provided by an adjustable fiberoptic light source (Fiber Lite, Series 180; Dolan-Jenner Instruments, Inc.) with a diffusion panel immediately below the bath. This light source was turned off during all experiments, except when used to induce photodynamic effects (see text). Irradiation measured at the axon was between 200 and 250 mW/cm² at the intensity settings used for photoexcitation of dye molecules. Spectral analysis of the light delivered to the axon showed a peak at 520 nm with half-maxima at 460 and 650 nm. Room lights were dimmed during control experiments using perfusates containing methylene blue.

Kinetic analysis of experimental records (see Starkus and Rayner, 1991) was carried out using either the OLIS KINFIT programs (On-Line Instrument Systems, Inc., Jefferson, GA) or, alternatively, the kinetic fitting routines of TempleGraph 2.4 (Mihalisin Associates, Inc., Ambler, PA). The two methods gave essentially identical results.

RESULTS

Removal of fast inactivation by MB + light

Fig. 1 demonstrates the principal findings of this study. Fig. 1 A shows the previously characterized effects of MB (0.5 mM) under low-illumination conditions. Note the lack of effect of MB on the initial gating currents and the similarity in the early rising phase of I_{Na} between trace *a* (initial control), trace *b* (during MB exposure), and trace *c* (after MB washout). However, trace *b* increasingly departs from the two control curves at times greater than about 200 μ s (at 0 mV test potential), indicating the time-dependent nature of the channel block induced by thiazin dyes. Under low ambient illumination the effects of MB are fully reversible, as seen by comparison of traces *a* and *c*. This axon was then re-exposed to the 0.5 mM MB perfusate (see Fig. 1 B), and the fiberoptic light source (see Materials and Methods) was turned on at the same intensity setting as was used during the dissection process. The initial effect of MB (not shown) was

a time-dependent block with kinetics similar to those seen in Fig. 1 A, trace *b*. During the ~ 15 -min illumination period, peak I_{Na} was progressively reduced (compare traces *b* in Fig. 1, A and B); however, washout of the MB solution reveals (see Fig. 1 B, trace *c*) that fast inactivation was almost completely removed during the 15-min period of MB + light exposure.

Table 1 shows the results of three-component exponential analysis of these traces. The analysis was initiated some 100 to 150 μ s after the start of depolarization, near the inflection point on the rising phase of sodium current, so as to avoid the initial delay in onset of I_{Na} . In this case, the fastest exponential component represents the major time constant of the I_{Na} rising phase (τ_a), the second component is the dominant time constant of fast inactivation in control traces (τ_{h1}), and the third component is the slower fast inactivation time constant (τ_{h2}). The analytical program also identified the asymptotic "steady-state I_{Na} " (I_{ss}) remaining after identification of these three major components. The control traces (*Aa*, *Ac*, and *Ba*) show essentially identical kinetics. Similarly, the two traces in the presence of MB (traces *Ab* and *Bb*) show the same τ_{h1} time constant as if, at this concentration of MB, early falling phase kinetics were determined by the kinetics of MB block irrespective of the presence (trace *Ab*) or absence (trace *Bb*) of the normal fast inactivation mechanism. The faster τ_a in the presence of MB does not necessarily imply that the intrinsic rate of channel activation is affected by drug action; it may simply reflect the effect of rapid open channel block on this "activation" eigenvalue. However, following washout of MB (trace *Bc*), τ_a is slowed and τ_{h1} is too small for detection by our analytical program (noted as not detectable in Table 1). Interestingly, the small residual fast inactivation present in this record has the time constant of τ_{h2} , as if this component of inactivation were relatively resistant to photodynamic damage. Possible causes of the slowing of τ_a following removal of fast inactivation, which appears as a consistent finding in later analyses (see Tables 2–5), will be considered in the Discussion.

Fig. 2 A explores the time course of these photodynamic effects. After initial control recordings to ensure axon stability (trace *a*), the axon was perfused with 0.5 mM MB, illuminated for 2 min, then washed with control perfusate and tested in a standard test pulse (from -120 mV to 0 mV) to assess the photodynamic effect of this illumination period (trace *b*). This process was repeated for each additional record (*c* through *e*), and cumulative illumination times preceding each test trace are given in the figure legend. Despite the continuing loss of sodium conductance throughout the illumination period, it is clear that steady-state conductance increases as fast inactivation is removed. Thus, the loss of fast inactivation is not due to selective removal of a fast inactivating channel population to expose a preexisting population of noninactivating channels. There must be a true conversion of channels from an inactivation-competent to an inactivation-incompetent form.

The nature of these kinetic changes is further explored in Fig. 2 B, where the same traces have been normalized to

FIGURE 1 Effects on inward sodium current of internal perfusion with 0.5 mM methylene blue, first under low ambient illumination (A) and then following photoexcitation (B). Comparing traces *a* and *c* in both panels, note the reversible time-dependent channel block in A, in contrast to the irreversible removal of fast inactivation and reduction in sodium current seen in B. Holding potential was -120 mV, and test potential was 0 mV for all traces. All data are from axon 910116. See text for further description of this experiment and Table 1 for kinetic analysis of these data traces.

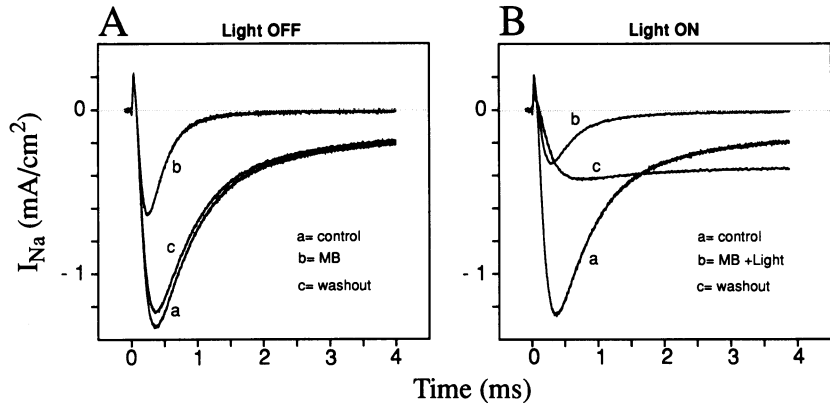


TABLE 1 Analysis of Fig. 1 data

Trace		τ_a (μ s)	τ_{h1} (μ s)	τ_{h2} (ms)	I_{Peak} (μ A/cm ²)	I_{ss} (μ A/cm ²)
Panel A						
Aa	Control	138	397	1.49	-1320	-166
Ab	MB	99	221	0.88	-633	-10
Ac	Washout	142	429	1.48	-1230	-154
Panel B						
Ba	Control	139	411	1.43	-1242	-155
Bb	MB + light	121	234	0.90	-325	-11
Bc	Washout	176	ND*	1.07	-422	-357

* ND, not detectable.

control peak I_{Na} . Note a slowing of activation rate concomitant with the loss of fast inactivation. Furthermore, loss of fast inactivation is complex, as shown in Table 2, which presents the results of three-component exponential analysis of the scaled data traces from Fig. 2 B. Neither the τ_{h1} nor τ_{h2} time constants change during fast inactivation removal, although the τ_{h1} intercept falls steadily while the τ_{h2} intercept initially increases (traces *a*–*d*). Relative reduction in the τ_{h2} intercept occurs only at long exposure times during the final stages of inactivation removal (see Fig. 2 B, trace *e*). (Note: Intercepts in Table 2 are zero time extrapolations, expressed as a percentage of normalized peak I_{Na} .)

The repeatability of these findings has been assessed (see Table 3) in a series of eight axons for which we have data traces showing incomplete fast inactivation removal after MB + light exposure. The mean data show a reduction in the τ_{h1} intercept to about 50% of its control level, that is, equivalent to an MB + light exposure time of around 5 min in the Table 2 data. Table 3 confirms (*a*) that photodynamic re-

moval of fast inactivation proceeds without apparent slowing of either τ_{h1} or τ_{h2} and (*b*) that the τ_{h1} intercept decreases before reduction in the τ_{h2} intercept can be detected. We have considered the possibility that variability of the time constants within this data set could be masking slowing of inactivation rates following MB + light exposure. However, we have not been able to detect significant trends in τ_{h1} or τ_{h2} values either from comparison of the means for the ratio “test t /control t ” in each axon or from rank-order tests of these ratios. (Intercepts in Tables 3, 4, and 5 were obtained from zero-time extrapolations, normalized as a percentage of the peak I_{Na} for each data trace.)

Although MB has been described as an inactivation simulator (Armstrong and Croop, 1982), our data clarify the hypothesis that photodynamic removal of fast inactivation does not remove the binding site for MB. For example, trace *b* of Fig. 1 B (which was obtained immediately prior to MB washout) shows that time-dependent block by MB has not been prevented by the removal of fast inactivation, which must already have been complete by that time. To follow up this question, we reintroduced MB (in the same axon as Fig. 1) at low ambient illumination. Fig. 3, trace *a*, shows complete removal of fast inactivation following the initial exposure to MB + light; trace *b* shows the time-dependent block produced following reintroduction of MB (without light); trace *c* shows the subsequent washout control, indicating the relative stability of the total sodium conductance in the absence of photodynamic effects. Subtraction of traces *b* and *c* gives a “difference current,” indicating the kinetics of onset of MB time-dependent block (see trace *d* of Fig. 3, and the similar difference current percentage block records shown for MB by Starkus et al., 1984, following removal of

TABLE 2 Analysis of scaled data from Fig 2B

Trace	MB + light (min)	τ_a (μ s)	τ_{h1} (μ s)	h1 intercept (% I_{Peak})	τ_{h2} (ms)	h2 intercept (% I_{Peak})	I_{ss} (% I_{Peak})
<i>a</i>	Control	105	383	165	1.45	24	5
<i>b</i>	2	103	352	123	1.30	40	15
<i>c</i>	4	120	424	92	1.75	39	31
<i>d</i>	6	141	385	49	1.28	49	51
<i>e</i>	16	182	ND*	ND	ND	ND	100

* ND, not detectable.

TABLE 3 Kinetic data from eight axons showing incomplete removal of fast inactivation

	τ_a (μ s)	τ_{h1} (μ s)	h1 intercept (% I_{Peak})	τ_{h2} (ms)	h2 intercept (% I_{Peak})	I_{ss} (% I_{Peak})
Control (means)	149	437	205	1.78	44	13
\pm SD	42	109	49	0.59	10	5
MB + light (means)	173	436	100	1.86	45	52
\pm SD	38	129	38	0.77	15	19

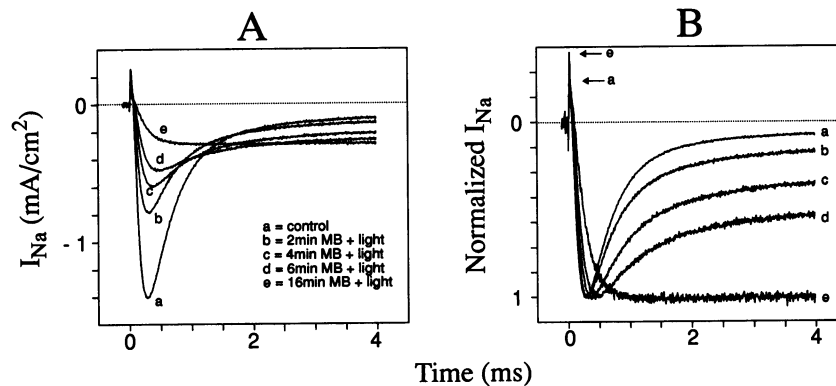


FIGURE 2 The time course of photodynamic fast inactivation removal during internal perfusion with 0.5 mM MB. (A) Unscaled data traces obtained at different times during MB + light exposure. Since time-dependent block by MB masks the inactivation processes, following an initial control (trace *a*) the axon was exposed to MB + light for a 2-min period and then washed free of internal MB in the dark before trace *b* was recorded. This protocol was repeated for each subsequent trace, yielding the cumulative exposure times shown for each trace (see *inset*). (B) Data traces from A normalized to control peak I_{Na} . Kinetic analysis of these traces is shown in Table 2. Horizontal arrows indicate gating current peak magnitudes for traces *a* and *e*; normalization of ionic currents does not yield equivalent normalization of the gating current traces. All data traces are from axon 910123; holding potential was -120 mV; test potential was 0 mV.

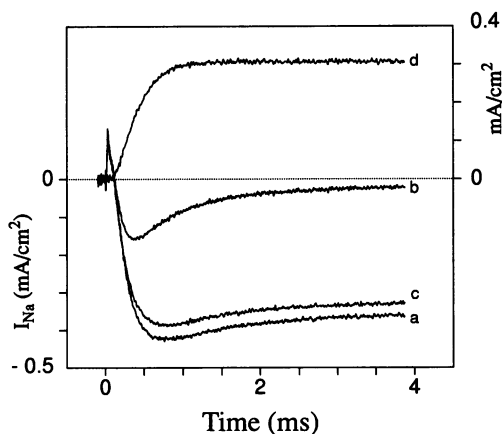


FIGURE 3 Photodynamic removal of fast inactivation does not affect the binding site for MB. Trace *a* shows the reference sodium current recorded after photodynamic removal of fast inactivation. The axon was then internally perfused with 0.5 mM MB at low ambient illumination (trace *b*). MB was then removed from the axon by washing with normal perfusate (trace *c*). Trace *d* is the “difference current” obtained by subtraction of traces *b* and *c*, indicating the time course of the reversible block by MB. All traces are from axon 910116 (the same axon as in Fig. 1); holding potential was -120 mV; test potential was 0 mV.

fast inactivation with pronase). The principal time constant for onset of MB block was 256μ s in trace *d*, which is very close to the τ_{h1} values from Table 1 in the presence of 0.5 mM MB. In this difference current note also the marked

sigmoid onset of channel block, consistent with the interpretation that the MB binding site is accessible only in fully open sodium channels.

Effects of MB + light on steady-state inactivation

Some part of the apparent loss of sodium conductance (after exposure to MB + light) could potentially result from the steady-state inactivation curve being “left-shifted” along the voltage axis, thus reducing sodium channel availability at holding potential. Fig. 4 A addresses this possibility, using methods described in detail by Ruben et al. (1992) to evaluate the effect of equilibrated (2 min) changes in holding potential on normalized sodium channel availability for the same axon before (*open boxes*) and after (*filled boxes*) exposure to MB + light. The control data (*open boxes*) are also compared with a previous control experiment (*open circles*) from Fig. 2A of Ruben et al. (1992) to indicate the repeatability of these steady-state inactivation curves in crayfish axons. First, the midpoint of the steady-state distribution has been shifted almost 20 mV to the right by MB + light, from -90 mV in the control curve (*open boxes*) to -72 mV after MB + light (*filled boxes*). Second, as noted also for the photodynamic effects of acridine orange on lobster axons by Pooler (1968), the slope of the “foot” of the curve has been substantially reduced. Steady-state inactivation curves in crayfish axons under control conditions were extensively investigated by Ruben et al. (1992), who noted a low-slope region (of $\sim 2.5e$)

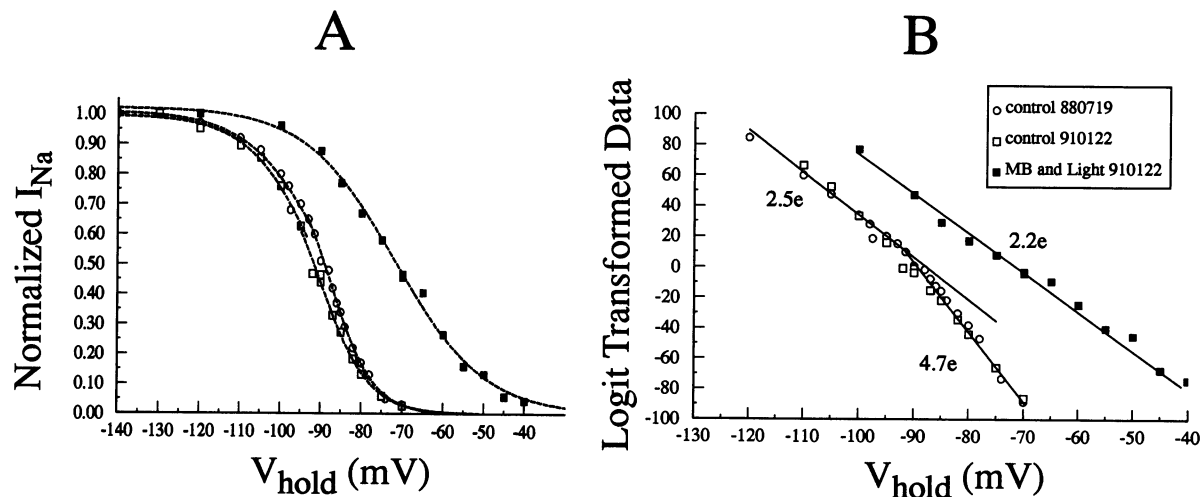


FIGURE 4 Normalized steady-state inactivation curves show that MB + light shifts the midpoint about 20 mV to the right along the voltage axis and reduces the slope of the curve. (A) Data from axon 910122 before (\square) and after (\blacksquare) photodynamic action. A control record from an earlier data set (axon 880719) is included to indicate the consistency of control measurements in these axons. All data points were obtained (as peak I_{Na} at 0 mV test potential) after 2 min at each holding potential; holding potentials changed in randomized order with return to reference holding potential (-120 V) after every two data points (see Ruben et al., 1992, for further details). (B) Logit transform of data from A.

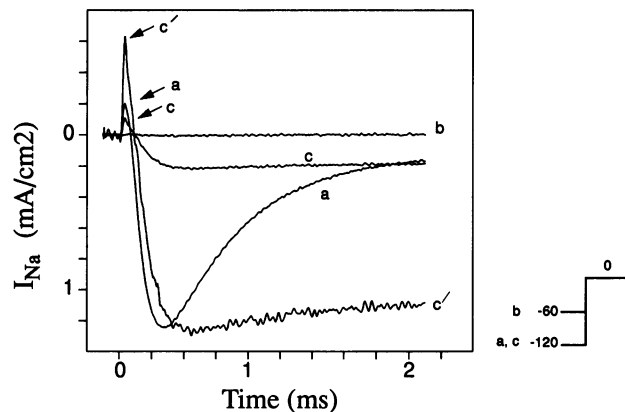


FIGURE 5 Steady-state inactivation does not protect against photodynamic removal of fast inactivation. Trace *a* shows the control sodium current in a step to 0 mV from -120 mV holding potential. Holding potential was then changed to -60 mV; sodium current was completely inactivated at this holding potential, and no inward current is visible in a step to 0 mV (trace *b*). The axon was then perfused with 0.5 mM MB and illuminated for 15 min. The MB was then washed out, and holding potential was returned to -120 mV. A subsequent test step to 0 mV (trace *c*) shows that inactivation was completely removed despite the depolarized holding potential. Trace *c'* shows this last record scaled to control peak I_{Na} ; note the disproportionate increase in peak gating current in the scaled *c'* record. All traces are from axon 91024.

at potentials more negative than -90 mV and a higher slope ($\sim 4e$) at more positive potentials. These changes in slope are more readily apparent after logit transform (see Fig. 4 B), where the control curve has slopes of $2.5e$ and $4.7e$. By contrast, the MB + light curve is well fitted by only a single slope of $2.2e \pm 0.1$ SD (assessing these data separately negative and positive to their midpoint voltage we obtained: $2.4e \pm 0.3$ SD and $2.7e \pm 0.4$ SD, respectively). Since neither the

right shift nor the reduction in slope would affect channel availability at -120 mV holding potential, the observed reduction in sodium conductance must result from some more direct effect of MB + light on sodium channels (see below).

After effective pronase treatment, the data of Bezanilla and Armstrong (1977) suggested that two channel types predominated: (i) channels with normal activation but no fast inactivation and (ii) “damaged” channels that neither conducted sodium ions nor generated gating current. Thus, they argued, scaling their data to match control I_{gON} should yield credible estimates of the “total” I_{Na} that would have been observed in the absence of any pronase-induced channel loss. By contrast, we find here that photodynamic reduction of peak sodium conductance is relatively greater than the loss of I_{gON} . Thus, when traces obtained following exposure to MB + light are scaled to control peak sodium conductance, their gating currents are always disproportionately large (usually about twofold greater than control I_{gON}). We demonstrate this scaling effect in Fig. 2 B (compare I_{Na} and I_{gON} peaks for traces *a* and *e*), Fig. 5 (traces *a* and *c'*), and Fig. 6 (traces *a* and *b*). Such findings suggest two alternative interpretations as to the channels remaining after photodynamic action; either (a) normal channels are present in proportions approximately equal to those of nonconducting channels which, nevertheless, generate normal gating currents, or (b) single-channel conductance has been reduced in some (or all) of the conducting channels. Data from single channel studies will be required to distinguish between these possibilities.

Exploring mechanisms of fast inactivation removal

We next consider a possible mechanism by which MB + light might modify fast inactivation. Armstrong and Croop

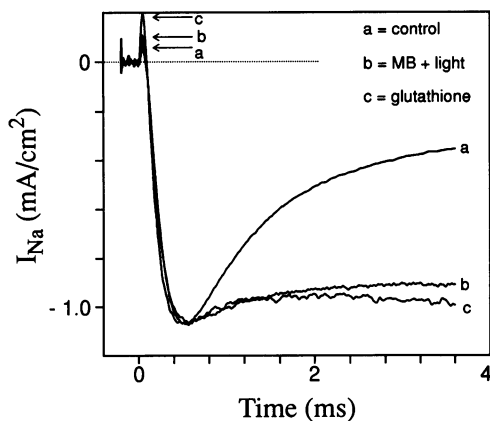


FIGURE 6 Glutathione (5 mM) fails to restore fast inactivation after photodynamic damage. Trace *a* shows the control sodium current; trace *b* (scaled ~ 2.5 -fold to match control peak I_{Na}) was taken after washout of MB, following 10 min of exposure to MB + light. Trace *c* (scaled ~ 5 -fold) shows a record taken after 5 min of perfusion with an internal perfusate containing 5 mM reduced glutathione. Horizontal arrows indicate the peaks of the gating currents in these scaled traces. All data are from axon 911008; holding potential was -120 mV, and test potential was 0 mV.

(1982) noted that, whereas fast inactivation retards the return of only the “immobilizable component” of gating charge, block by thiazine dyes additionally immobilizes the normally “nonimmobilizable” component of I_{gOFF} . Similarly, previous studies of MB block (see Starkus et al., 1984) have shown that the binding of such agents seems more voltage sensitive ($0.85e$) than the onset of fast inactivation ($0.4e$) (Stimers et al., 1985). In the context of the “ball-and-chain model” (Armstrong and Bezanilla, 1977), these findings suggest that the MB binding site may be deeper into the channel than the binding site for the fast inactivation ball. Thus, the apparent competition reported between fast inactivation and MB binding (Starkus et al., 1984) may be steric rather than indicative of a common receptor site. We therefore explored the possibility that the binding site for fast inactivation might be superficial enough to be damaged by MB + light action, even at strongly negative holding potentials. If destruction of the fast inactivation binding site is the major mechanism of photodynamic fast inactivation removal, then inducing both fast and steady-state inactivation by holding the axon at a relatively depolarized potential (-60 mV) should offer some protection against this action of MB + light.

Fig. 5 shows two control traces obtained in steps to the same test potential (0 mV) from different holding potentials. Holding potential was -120 mV for trace *a* and -60 mV for trace *b*.

Note that sodium conductance is completely inactivated at -60 mV holding potential. The 0.5 mM MB perfusate was then introduced while continuing to hold the axon at -60 mV; the light was then turned on for 10 min while the axon remained unstimulated; after turning off the light, MB was washed out using the control internal perfusate. Holding potential was then returned to -120 mV, and trace *c* was obtained in a test step to 0 mV. This trace shows that fast inactivation was effectively removed by our standard MB +

light exposure regimen, despite the depolarized holding potential and evident prior inactivation of sodium channels.

Recently, Ruppertsberg et al. (1991) reported that fast inactivation can be regulated by oxidation/reduction of a cysteine residue in the “ball domain” present in the NH_2 -terminus region of fast inactivating, A-type, potassium channels. Normal fast inactivation depends on this cysteine remaining in its reduced condition. The authors speculate that disulfide bond formation cross-links the ball domain to some other part of the channel molecule following oxidation of the critical cysteine residue. They found that exposure of the internal surface of their patch to 5 mM reduced glutathione solution was sufficient to reverse the removal of fast inactivation that they had observed in normal artificial media. Since photoreduction of MB at near-mM concentrations has been reported to generate H_2O_2 in aqueous solutions (see Somer and Green, 1973), we had suspected that disulfide bond formation might also be involved in the removal of fast inactivation by MB + light. Such a finding would suggest the presence of an exposed cysteine residue in the sodium channel ball domain and assist in characterization of this functional component at the structural level. Unfortunately, we found no restorative effects on fast inactivation during perfusion with reduced glutathione at either 5 or 10 mM. Fig. 6 demonstrates this negative result. Trace *a* shows the control sodium current; trace *b* demonstrates the removal of fast inactivation following a 10-min exposure to MB + light (this trace has been scaled ~ 2.5 -fold to match control current magnitude); trace *c* shows the sodium current after a 5-min perfusion with 5 mM reduced glutathione perfusate (record scaled ~ 5 -fold) to match control current magnitude.

Carotenoid protection against photodynamic damage

Oxford et al. (1977) described a protective effect of β -carotene on the photodynamic reduction in sodium and potassium conductance following exposure to MB + light. The protocol used by Oxford et al. involved a 30-min pre-exposure to a saturated solution of β -carotene, followed by a 3-min perfusion with β -carotene plus 100 mM MB. Illumination for 2 min in the presence of both β -carotene and MB produced only minimal changes in sodium and potassium conductance. By contrast, a substantial loss of current occurred after only 30 s of additional illumination in MB alone (following a 5-min washout of the β -carotene). We were interested in seeing whether carotenoids would similarly protect against both photodynamic removal of fast inactivation and right shifting of the steady-state inactivation curve. However, carotenoids are highly insoluble in water and may well partition into the membrane lipids during the 30-min pretreatment period. Thus, the protocol used by Oxford et al. (1977) could not clarify whether protective action results from quenching in solution or from carotenoid molecules taken up by the membrane. This question is clarified in Fig. 7 (traces *a*, *b*, and *c*). Trace *a* shows the sodium current under control conditions; trace *b* shows kinetic changes oc-

TABLE 4 Analysis of traces from Fig. 7

Trace		τ_a (μ s)	τ_{h1} (μ s)	h1 intercept (% I_{Peak})	τ_{h2} (ms)	h2 intercept (% I_{Peak})	I_{ss} (% I_{Peak})
<i>a</i>	Control	139	641	151	3.68	14	5
<i>b</i>	Carotenoid	138	449	181	1.92	20	5
<i>c</i>	Wash	129	442	182	2.55	14	4
<i>d</i>	MB + light	100	244	235	1.23	17	3
<i>e</i>	Wash	132	503	61	3.22	31	48

TABLE 5 Kinetic data from six axons pretreated with carotenoids

	τ_a (μ s)	τ_{h1} (μ s)	h1 intercept (% I_{Peak})	τ_{h2} (ms)	h2 intercept (% I_{Peak})	I_{ss} (% I_{Peak})
Carotenoid (means)	111	430	218	2.30	21	4
\pm SD	34	85	50	0.71	11	2
MB + light (means)	143	446	144	2.43	37	39
\pm SD	33	202	73	0.82	7	15

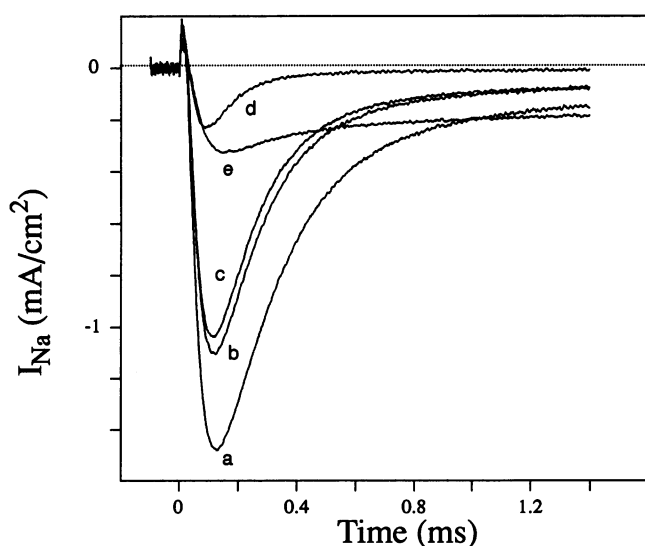


FIGURE 7 Pre-exposure to carotenoids modifies sodium current kinetics and slows the removal of fast inactivation by MB + light. Trace *a* shows control sodium current; trace *b* was taken during a 30-min pre-exposure to canthaxanthin; trace *c* was obtained 15 min after washout of carotenoid from the internal perfusate. Note that there is no return to control kinetics after carotenoid washout. Trace *d* was taken following a 20-min exposure to MB + light, and trace *e* shows the partial removal of fast inactivation achieved following pre-exposure to the carotenoid. Data are from axon 920914; holding potential was -120 mV, test potential was 0 mV. Kinetic analysis of these traces is presented in Table 4.

curing at the start of a 30-min exposure to 10 mM canthaxanthin perfusate (solubilized using tetrahydrofuran; see Materials and Methods). Finally, in trace *c*, we show that these changes persist despite a 15-min washout in carotenoid-free perfusate. Table 4 shows the results of kinetic analysis of these traces; we have found significant reductions for both τ_{h1} and τ_{h2} associated with carotenoid exposure, in all axons in which this protocol was used. Although the kinetic effects are similar to those produced by time-dependent blocking agents, such effects would not persist unchanged throughout a 15-min washout period. We presume that the

kinetic changes of traces *b* and *c* most probably result from uptake of the highly lipophilic carotenoid molecules either into the channel molecule itself or into closely adjacent regions of the lipid bilayer. The alternative possibility, that carotenoids produce a permanent chemical modification of the sodium channel, which both changes kinetics and protects against MB + light action, seems lacking in appropriate parsimony.

The axon was then perfused with 0.5 mM MB + light for 20 min (trace *d*) and washed free of MB perfusate (trace *e*). Although Fig. 7 provides no evidence of reduction in channel loss after carotenoid exposure, some protection is evident against the removal of fast inactivation. Comparison with Table 2 shows a similar $\sim 50\%$ loss of fast inactivation after a 6-min exposure to MB + light in the absence of carotenoid and after 20 min in presence of carotenoid. The lack of carotenoid protection against channel loss was confirmed in a series of carefully matched experiments. Mean suppression was 65% ($\pm 15\%$ SD, $n = 6$) for peak I_{Na} and 41% ($\pm 8\%$) for peak I_g in MB + light by comparison with 63% ($\pm 6\%$ SD, $n = 5$) for peak I_{Na} and 34% ($\pm 6\%$) for peak I_g after pre-exposure to carotenoid. The mean illumination period was 14 min (± 3 SD) in the MB + light experiments and 14 min (± 2 SD) for the carotenoid-exposed axons.

We have further explored the repeatability of the Fig. 7 data by kinetic analysis of a series of six axons in which MB + light exposure occurred following carotenoid pretreatment (see Table 5).

Here the "carotenoid" data were obtained following washout (cf. trace *c* in Fig. 7 and Table 4), and the MB + light data were obtained after washout of the MB (cf. trace *e* in Fig. 7 and Table 4). Although the time constant of activation appears slowed by the removal of fast inactivation, there are no changes in either τ_{h1} or τ_{h2} . Additionally, the τ_{h1} intercept becomes reduced before similar changes appear in the intercept for τ_{h2} .

Fig. 8 explores carotenoid protection (here using 10 mM lycopene) against the effects of MB + light on steady-state inactivation. We first obtained a control steady-state curve

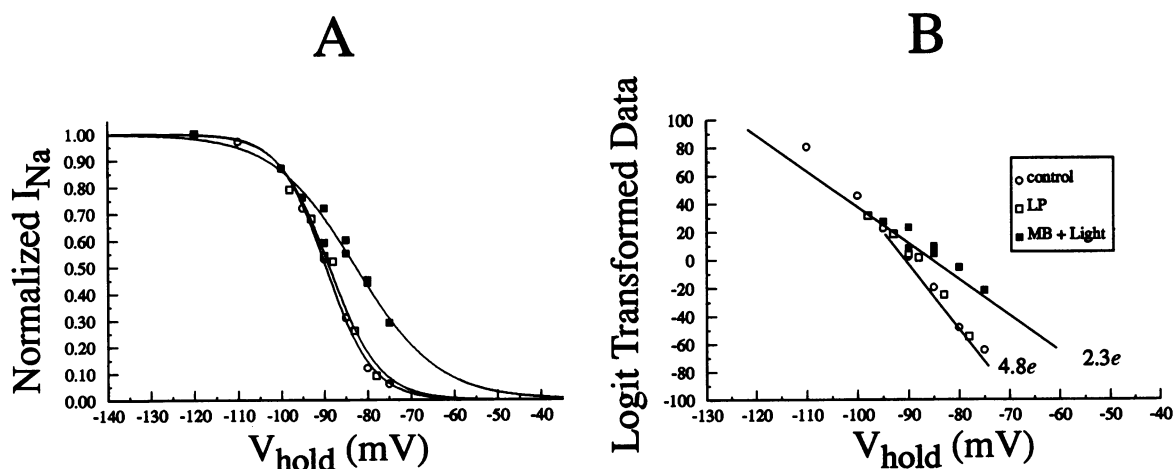


FIGURE 8 Pre-exposure to carotenoids reduces the right shifting of the steady-state inactivation curve. (A) The control steady-state inactivation curve (\circ) was obtained as described for Fig. 4. The axon was then perfused with lycopene for a total of 90 min, and a second curve (\square) was generated. After lycopene washout, the axon was exposed to MB + light for 15 min and washed free of MB. The curve obtained after MB + light exposure (\blacksquare) shows reduced slope. However, the right shift is markedly reduced by comparison with the corresponding curve in Fig. 4, which was obtained without carotenoid pretreatment. All data are from axon 920922. Test potential was 0 mV, and reference holding potential was -120 mV. (B) Logit transform of data from A.

(Fig. 8 A, open boxes) as described for Fig. 4. This protocol was repeated during exposure to 10 mM lycopene, showing no significant effect of lycopene on the steady-state inactivation curve (Fig. 8 A, open circles). The total time of exposure to lycopene was about 90 min (due to the time-consuming nature of this protocol with its multiple changes in holding potential). The axon was then washed for 15 min in control perfusate and exposed for 15 min to MB + light. After washout of MB, a final curve was obtained (Fig. 8 A, filled boxes). The slopes of these curves were evaluated after logit transform (see Fig. 8 B). The midpoint for the control curve was -88 mV versus -83 mV for MB + light following carotenoid exposure, showing substantial protection by comparison with the 18 mV right shift seen in Fig. 4. However, the effective valence for the MB + light curve was $2.3e$ ($\pm 0.2e$ SD) with pre-exposure to carotenoid versus $2.2e$ (± 0.1 SD) for the comparable curve obtained without carotenoid exposure (see Fig. 4), indicating no significant protection against the reduction in effective valence. In a series of five axons, MB + light produced a mean right shift of only 1.4 mV (± 4.0 mV, SD) following carotenoid exposure. The MB + light-induced right shift was 16.5 mV (± 5.0 mV, SD) in a control series of axons without prior carotenoid exposure.

To assess the importance of direct quenching of reactive species by dissolved carotenoids in the perfusate, we compared the above data with results of experiments in which (after a similar pre-exposure to the carotenoid) both carotenoid and MB were present in the internal perfusate during light exposure. We found no additional protection from the dissolved carotenoids under our experimental conditions.

DISCUSSION

For crayfish axonal sodium channels, the principal photodynamic effects observed after internal perfusion with so-

lutions containing 0.5 mM MB are (i) suppression of maximum conductance, (ii) right shifting of the steady-state inactivation curve, (iii) reduction in the effective valence of the steady-state inactivation curve, and (iv) progressive removal of fast inactivation without change in inactivation rates, although (v) the intercepts of the two fast inactivation relaxations (τ_{h1} and τ_{h2}) are differentially affected by MB + light. These last two findings differ from the conclusions of previous work (Pooler, 1968; Pooler, 1972; Pooler and Oxford, 1973; Oxford et al., 1977), which reported slowing of fast inactivation following photodynamic damage. However, the apparent conflict may arise from differences in analytical methods rather than from significant differences in the data, since only single-exponential analysis was used in the previous work (apparently without subtraction of steady-state asymptotes). Thus, a relative increase in steady-state I_{Na} (clearly visible in the earlier data and specifically noted by Oxford et al., 1977) would produce an apparent slowing of a single inactivation time constant.

The present study has made no attempt to clarify the dose-effect relationships of photodynamic action. The effective "dose" reflects the concentrations of multiple reactive species in the region immediately below the axonal membrane and will depend on both dye concentration and light intensity in complex ways. Thus, when light is applied from a directional source, increasing MB concentration will reduce the penetration of light and may even reduce the total production of reactant species (see Somer and Green, 1973). We chose here to use a concentration of MB that gives near-maximal channel block under dark conditions and then used a light intensity low enough to require >10 min MB + light exposure to produce a full removal of fast inactivation. These conditions facilitate exploration of the onset of fast inactivation removal, which was the original focus of this study. However, in view of the light absorption by 0.5 mM MB, the directional illumination used here necessarily creates differ-

ences in effective illumination “dose” at different points around the circumference of the axon.

Selective protection by carotenoids

Krinsky (1979) has reviewed the three principal mechanisms by which carotenoids may affect photodynamic damage produced by exogenous dyes: (i) direct quenching of the excited triplet state (3S) of the photosensitizing dye; (ii) quenching of highly reactive singlet oxygen (1O_2) produced by interaction between triplet 3O_2 and 3S ; (iii) destructive interactions between carotenoids and free radicals produced by excited singlet (1S) or 3S dye molecules. It does not seem appropriate to assume that all protective effects of carotenoids are necessarily mediated by quenching of 1O_2 , and the relative importance of these three interactive processes will depend on the concentrations and characteristics of the dye and carotenoid pigments involved, as well as on the nature of the solvent in which the reactions take place. Although Foote and Denny (1968) demonstrated that β -carotene prevents MB-induced photooxidation by quenching 1O_2 (with direct quenching of the 3S state occurring only when β -carotene is present in very much higher concentration than MB), this study was carried out in benzene:methanol (80:20 mixture) with 2-methyl-2-pentene as the photooxygenation acceptor. In acidic aqueous solution (Somer and Green, 1973), photoreduction of MB appears to proceed via a relatively long-lived excited intermediate, to yield the colorless reduced MB and H_2O_2 . However, such studies may have little relevance to experiments in which the photoexcitation occurs in neutral aqueous solution and where the carotenoid is apparently sequestered within, or very close to, the sodium channel molecule (see Fig. 7 and Table 4). We have therefore concentrated on the insights our results may provide as to the mechanistic complexity of the fast and steady state inactivation processes.

Nevertheless, we have been concerned by our inability to demonstrate effective protection by carotenoids against photodynamic channel loss, as has been reported by Oxford et al. (1977). It seems most probable that our different result arises from our choice of higher MB concentration and markedly lower light intensity. Their experimental conditions may have favored the production of different reactive species, which might be more susceptible to quenching from solution.

Implications of MB + light effects

During the initial phase of MB + light exposure (between 2 and 6 min in Fig. 2) the principal effect is a marked reduction in the intercept for τ_{h1} , coincident with a small relative increase in the intercept for τ_{h2} . Thereafter (i.e., between 6 and 16 min in Fig. 2) the intercepts for both components become reduced to undetectable levels. Similarly, in the mean data of Table 3 the τ_{h1} intercept is markedly reduced without apparent change in the τ_{h2} intercept in these axons with incomplete inactivation removal. Thus, in Table 1 (trace Bc), where inactivation is almost completely removed, the small

remnant of fast inactivation shows only the τ_{h2} rate. That the τ_{h1} and τ_{h2} intercepts are differentially affected by MB + light, without significant change in either eigenvalue, suggests the conclusion that τ_{h1} and τ_{h2} must reflect noninteracting processes with different susceptibilities to photodynamic damage.

Unfortunately, our present results fail to clarify the origins of these two inactivation processes. Both the τ_{h1} and τ_{h2} mechanisms appear “fast” by comparison with the kinetics of drug-resistant slow inactivation (Rudy, 1978; see also Starkus and Rayner, 1991). Similarly, both are susceptible to photodynamic action and both seem protected to similar extents by prior carotenoid exposure. Two separate sodium channel populations with different fast inactivation kinetics might be expressed in the crayfish axonal membrane, despite our previous work, which failed to provide direct evidence for this interpretation (see Ruben et al., 1990). Alternatively, the separate kinetics might arise from interconverting kinetic subpopulations within the same channel type (cf. Moorman et al., 1990). For example, it seems possible that τ_{h1} reflects fast inactivation in “fast mode” channels, whereas τ_{h2} reflects the altered kinetics of the same fast inactivation mechanism operating in the “slow mode” channel conformation. Where these gating modes reflect different conformational states of the same channel type, the inactivation mechanism may be more susceptible to photodynamic damage in the fast mode channel conformation. Additionally, photodynamic effects might reduce the τ_{h1} intercept by favoring conversions from fast to slow mode. We have noted a relative increase in τ_{h2} intercept (see Table 2) during MB + light exposure, which is accompanied by both reduction in the τ_{h1} intercept and substantial channel loss. It is thus not yet clear whether our data support an absolute increase in τ_{h2} sufficient to indicate conversion of channels from τ_{h1} to τ_{h2} behavior. However, we have noted a consistent slowing of τ_a after MB + light exposure (see Tables 1–5). This finding is predicted by the hypothesis that MB + light causes a conversion of channels from fast to slow gating mode. Extending our study to include cloned channels should help to clarify this hypothetical mechanism.

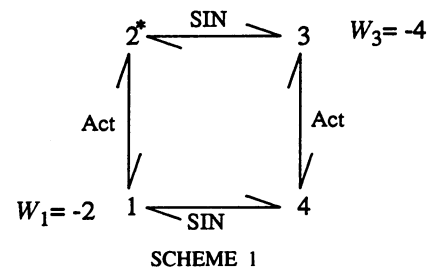
Although our results distinguish two kinetically and pharmacologically separable components of fast inactivation, they provide little insight into the underlying mechanism by which fast inactivation occurs in sodium channels. Removal of inactivation is not reversible by glutathione (Fig. 6) and continues despite prior inactivation of sodium channels by holding the membrane at -60 mV, where channels are fully inactivated under control conditions (see Figs. 4 and 5). If we could assume that the binding sites for the fast inactivation balls would be protected by prior inactivation, we could conclude that MB + light modifies some more readily accessible component of the fast inactivation mechanism. However, there are problems with this interpretation. First, although strong evidence supports the “ball-and-chain” mechanism in A-type potassium channels (Hoshi et al., 1990), there is as yet no similarly unequivocal evidence to support this mechanism in sodium channels (although it remains a reasonable

working hypothesis). Second, channels may be primarily slow inactivated, rather than fast inactivated, under steady-state conditions (although, if these are parallel processes both may occur in steady state). Third, supposing that the right shifting of the steady-state inactivation curve may occur as the initial photodynamic action in at least some channels (see below), it remains possible that many channels would eventually cycle through the activatable state even at -60 mV (and so lose protection for their fast inactivation binding sites). If such cycling of channels into unprotected states was the rate-limiting process at -60 mV holding potential, then removal of fast inactivation would be slower and markedly less complete at -60 mV than at -120 mV; we observed no such effect. Thus, removal of both the τ_{h1} and τ_{h2} fast inactivation processes would seem to involve effects on the hypothesized ball and chain rather than on the inactivation binding site.

Carotenoid exposure separates two different effects of MB + light on the steady-state availability of sodium channels (as seen after 2-min equilibrations at each holding potential). As shown in Fig. 8, carotenoids seem to reduce the right shift of the midpoint of the steady-state inactivation curve but fail to protect against the loss of the high-slope region at the foot of this curve. It is important to remember that these experimental protocols assess the fully equilibrated steady-state availability of sodium channels. In contrast to "h_∞ curves" obtained using short (2–15 ms) prepulses (see Ruben et al., 1992), the steady-state curve in crayfish axons is left shifted by about 40 mV and shows a high-slope region absent from the h_∞ distribution. Ruben et al. (1992) argued on kinetic grounds that fast inactivation was not a major contributor to steady-state inactivation, although removal of fast inactivation by pronase and *N*-bromoacetamide is well known to result in a ~ 20 mV right shift of the steady-state inactivation curve (e.g., see Heggeness and Starkus, 1986). However, Starkus and Shrager (1978) demonstrated that trypsin also right-shifts steady-state inactivation by about 20 mV in crayfish axons, without removal of fast inactivation. Here we show the inverse of that result: that is, removal of fast inactivation (following prior carotenoid exposure) can occur without substantial right-shifting of steady-state inactivation (see Fig. 8). Clearly, the right-shifting of steady-state inactivation is not merely a consequence of removing an "absorbing" fast inactivated state (as would be predicted from simple sequential models). Similarly, the loss of the high-slope region of the steady-state inactivation curve following MB + light exposure appears to be a specific consequence of photodynamic action and does not occur during right-shifts of the midpoint induced by pronase, trypsin, chloramine-T or *N*-bromoacetamide (Starkus et al., 1993b). Removal of fast inactivation, right-shifting of steady-state inactivation, and removal of the high-slope region at the foot of the steady-state inactivation curve are apparently independent effects that must, therefore, be mediated by different structural changes in the sodium channel molecule.

The present study thus provides additional support for the simple four-state model introduced by Bezanilla et al. (1982) and modified by Ruben et al. (1992) (see Scheme I, below).

In this model the voltage sensitivity of activation (Act) becomes shifted to the left as the steady state is approached, through electrostatic coupling to slow inactivation (SIN). As pointed out by Ruben et al. (1992), if SIN is an inherently voltage-sensitive process, both the slow inactivation and activation valences will contribute to the apparent valence of steady-state inactivation (explaining the low- and high-slope regions in the steady-state inactivation curve). Fig. 9 shows logit transforms of simulated steady-state inactivation curves, demonstrating that this coupled parallel model can describe not only the control curve but also its modification by photodynamic effects (cf. Fig. 4) and carotenoid protection (cf. Fig. 8), following appropriate changes in specific model parameters (see text and Scheme II, below).



Simulation of photodynamic effects on steady-state inactivation

1. Simulation of control data

In Scheme I, position 1 represents the "resting" closed state, position 2* is the open state, and positions 4 and 3 are comparable slow inactivated states. Well-to-barrier heights are specified for the hyperpolarization-favored (ω_a) and depolarization-favored (ω_b) energy wells in kT units, and valences (z) and barrier positions (d) are shown in Table 6 for each set of transitions. Cooperative coupling between activation and slow inactivation is specified as a change in well energy (W_a or W_b) following the approach introduced by Bezanilla et al. (1982). Thus the attraction between the activation and slow inactivation particles effectively increases well-to-barrier height. Models specified in this manner necessarily comply with requirements of microscopic reversibility, despite the apparently asymmetrical distribution of coupling energies. Reaction rates were calculated using the modified rate equations of Bezanilla et al. (1982). Thus, where K_α is the rate constant of the depolarization-favored transition and K_β is the hyperpolarization-favored back reaction rate, then

$$K_\alpha = (kT/h) \cdot \exp([W_a - \omega_a + ezd V]/kT)$$

$$K_\beta = (kT/h) \cdot \exp([W_b - \omega_b - ez(1 - d)V]/kT)$$

where e is the electronic charge, V is the membrane potential, k is the Boltzmann constant, h is Planck's constant, and T is the absolute temperature.

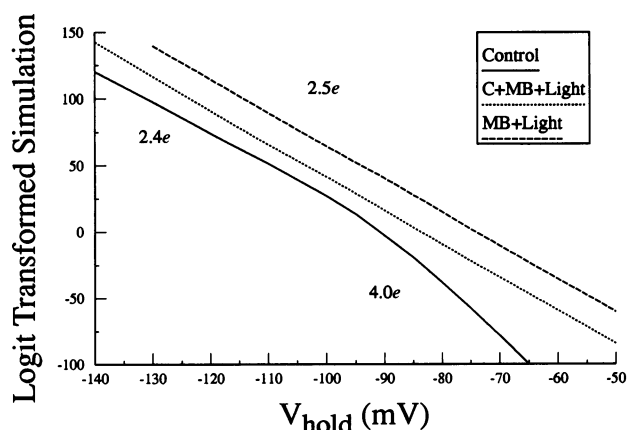


FIGURE 9 Logit transformation of simulated steady-state inactivation curves for comparison with experimental data (see inset). The *Control* simulation (—) was obtained using the Scheme I model (see text and Table 6 for model parameters). This curve shows a midpoint of -90 mV and two slopes comparable to those found in control data curves (cf. the control curves in Figs. 4 B and 8 B). The two curves simulating effects of photodynamic damage were obtained using the Scheme II model in which slow inactivation is presumed to be voltage insensitive. The simulation of the unprotected actions of MB + light (---) should be compared with data shown in Fig. 4 B. This curve shows a slope of $2.5e$ and a midpoint of -74 mV. The protective effect of carotenoids (....., C + MB + light) should be compared to the equivalent data in Fig. 8 B. The slope is $2.5e$, with a midpoint of -84 mV.

TABLE 6 Simulation parameters for Scheme I model

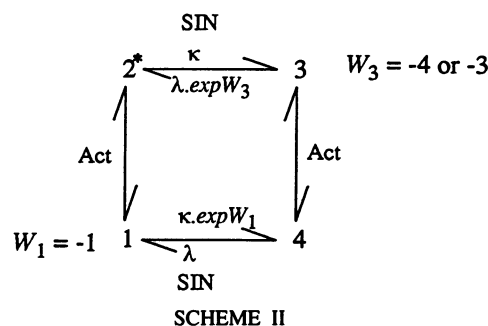
Transition	W_a	ω_a	W_b	ω_b	z	d
1,2	-2	19	0	24.2	2.5	0.5
4,3	0	19	-4	24.2	2.5	0.5
1,4	-2	25	0	34	2.0	0.5
2,3	0	25	-4	34	2.0	0.5

The simulations for the logit transformed control curve (see Fig. 9) were obtained exactly as described in Ruben et al. (1992). However, both the well-to-barrier heights and the valences (see Table 6) were modified slightly from the parameters used by Ruben et al. (1992), to improve the fit to our data. The measured effective valences for this simulated control curve were $2.4e$ in the low-slope region and $4.0e$ in the high-slope region, with a midpoint of -90 mV.

2. Simulation of photodynamic effects

In the Scheme I model discussed above, the high-slope region derives from the independent voltage sensitivity of the SIN reactions, whereas the midpoint of the steady-state curve is determined by the strength of the coupling between the activation and slow inactivation processes. Thus the effects of MB + light on the steady-state inactivation curve (right shifting of the midpoint with loss of the high-slope region) suggest that (a) coupling becomes less effective and (b) the SIN mechanism loses its voltage sensitivity (see Scheme II). In Scheme II the 1,4 and 2,3 (SIN) reactions are described by the voltage-insensitive reaction rates κ and λ , with coupling energies included for the 1–4 reaction as $\kappa \cdot \exp W_1$ and

for the 3–2 reaction as $\lambda \cdot \exp W_3$. Since slow inactivation remains complete at positive holding potentials, these reactions were biased in the direction of the closed slow inactivated state, setting κ as $0.000004 \mu\text{s}^{-1}$ and λ as $0.000001 \mu\text{s}^{-1}$. An acceptable simulation of our MB + light data was obtained with the reduction of W_1 from -2 to -1 and W_3 from -4 to -3 kT units without any other parameter changes (see Fig. 9). The effects of carotenoid pretreatment can then be modeled as a smaller change in the coupling factors, by lowering only W_1 (from -2 to -1). It should be noted, however, that these simulations assume “saturation” of the cumulative effects of MB + light on individual channels has occurred during our treatment protocols, yielding reasonably uniform populations of drug-modified channels. Additional work will be required to assess the validity of that assumption.



Despite the highly simplified nature of Schemes I and II, such models suggest reasonable physical interpretations for the effects of photodynamic action on steady-state inactivation. Furthermore, the prediction that slow inactivation becomes voltage insensitive following photodynamic damage by MB + light can be subjected to direct experimental testing. Confirmation of this prediction would suggest a resolution of the apparent distinction between “voltage-sensitive slow inactivation,” typical of sodium channels and “voltage insensitive slow inactivation,” associated with the carboxy-terminal region of Shaker potassium channels (Zagotta et al., 1991). Additionally, such a finding would suggest that slow inactivation is controlled by a relatively exposed, presumably “non-S4” voltage sensor (rather than being directly controlled by one of the S4 segments, as suggested by Ruben et al., 1992). A negatively charged, non-S4 voltage sensor for slow inactivation would provide a simple electrostatic mechanism to explain our hypothesized cooperative coupling to positively charged, activating, S4 voltage sensors.

This study was supported by National Institutes of Health grants to J. G. S. (RO1 NS21151) and P. C. R. (RO1 NS29204). Additional support was received through grants-in-aid from the American Heart Association (Hawaii Affiliate) to J. G. S. and P. C. R., as well as from a Research Centers at Minority Institutions award (3G12RR03061) and a Biomedical Research Support grant (2S07RR07026).

REFERENCES

Alicata, D. A., M. D. Rayner, and J. G. Starkus. 1989. Osmotic and pharmacological effects of formamide on capacity current, gating current, and

- sodium current in crayfish giant axons. *Biophys. J.* 55:347–353.
- Armstrong, C. M., and F. Bezanilla. 1977. Inactivation of the sodium channel. II. Gating current experiments. *J. Gen. Physiol.* 70:567–590.
- Armstrong, C. M., and R. S. Croop. 1982. Simulation of Na channel inactivation by thiazin dyes. *J. Gen. Physiol.* 80:641–662.
- Bezanilla, F., and C. M. Armstrong. 1977. Inactivation of the sodium channel. I. Sodium current experiments. *J. Gen. Physiol.* 70:549–566.
- Bezanilla, F., R. E. Taylor, and J. M. Fernandez. 1982. Distribution and kinetics of membrane dielectric polarization. I. Long-term inactivation of gating currents. *J. Gen. Physiol.* 79:21–40.
- Croop, R. S., and C. M. Armstrong. 1979. Dark effects of dyes in perfused squid axons (Abstract). *Biophys. J.* 25:13a.
- Fleig, A., M. Sadeghpour, and J. G. Starkus. 1992. Fast inactivation: removal by photodynamic action of methylene blue (Abstract). *Biophys. J.* 61:618a.
- Foote, C. S., and R. W. Denny. 1968. Chemistry of singlet oxygen. VII. Quenching by b-carotene. *J. Am. Chem. Soc.* 90:6233–6235.
- Heggeness, S. T., and J. G. Starkus. 1986. Saxitoxin and tetrodotoxin. Electrostatic effects on sodium channel gating current in crayfish giant axons. *Biophys. J.* 49:629–643.
- Hoshi, T., W. N. Zagotta, and R. W. Aldrich. 1990. Biophysical and molecular mechanisms of Shaker potassium channel inactivation. *Science (Washington DC)*. 250:533–538.
- Krinsky, N. I. 1979. Carotenoid protection against oxidation. *Pure Appl. Chem.* 51:649–660.
- Moorman, J. R., G. E. Kirsch, A. M. J. Van Dongen, R. H. Joho, and A. M. Brown. 1990. Fast and slow gating of sodium channels encoded by a single mRNA. *Neuron*. 4:243–252.
- Oxford, G. S., J. P. Pooler, and T. Narahashi. 1977. Internal and external application of photodynamic sensitizers on squid giant axons. *J. Membr. Biol.* 36:159–173.
- Pooler, J. P. 1968. Light-induced changes in dye-treated lobster giant axons. *Biophys. J.* 8:1009–1026.
- Pooler, J. P. 1972. Photodynamic alteration of sodium currents in lobster axons. *J. Gen. Physiol.* 60:367–387.
- Pooler, J. P., and G. S. Oxford. 1973. Photodynamic alteration of lobster giant axons in calcium-free and calcium-rich media. *J. Membr. Biol.* 12:339–348.
- Rayner, M. D., and J. G. Starkus. 1989. The steady-state distribution of gating charge in crayfish giant axons. *Biophys. J.* 55:1–19.
- Ruben, P. C., J. G. Starkus, and M. D. Rayner. 1990. Holding potential affects the apparent voltage-sensitivity of sodium channel activation in crayfish giant axons. *Biophys. J.* 58:1169–1181.
- Ruben, P. C., J. G. Starkus, and M. D. Rayner. 1992. Steady-state availability of sodium channels. Interactions between activation and slow inactivation. *Biophys. J.* 61:941–955.
- Rudy, B. 1978. Slow inactivation of the sodium conductance in squid giant axons. Pronase resistance. *J. Physiol. (Lond.)*. 283:1–21.
- Ruppersberg, P. J., M. Stocker, O. Pongs, S. H. Heinemann, R. Frank, and M. Koenen. 1991. Regulation of fast inactivation of cloned mammalian I_k (A) channels by cysteine oxidation. *Nature (Lond.)*. 352:711–714.
- Shrager, P. 1974. Ionic conductance changes in voltage clamped crayfish axons at low pH. *J. Gen. Physiol.* 64:666–690.
- Somer, G., and M. E. Green. 1973. Photoreduction of methylene blue by water. *Photochem. Photobiol.* 17:179–190.
- Starkus, J. G., and M. D. Rayner. 1991. Gating current “fractionation” in crayfish giant axons. *Biophys. J.* 60:1101–1119.
- Starkus, J. G., and P. Shrager. 1978. Modification of slow sodium inactivation in nerve after internal perfusion with trypsin. *Am. J. Physiol.* 4:C238–C244.
- Starkus, J. G., S. T. Heggeness, and M. D. Rayner. 1984. Kinetic analysis of sodium channel block by internal methylene blue in pronased crayfish giant axons. *Biophys. J.* 46:205–218.
- Starkus, J. G., A. Fleig, M. D. Rayner, and P. C. Ruben. 1993a. Dissecting fast inactivation removal: 2) Photodynamic effects (Abstract). *Biophys. J.* 64:87a.
- Starkus, J. G., M. D. Rayner, and P. C. Ruben. 1993b. Dissecting fast inactivation removal: 1) Effects of internal pH and chemical modifiers (Abstract). *Biophys. J.* 64:87a.
- Stimers, J. R., F. Bezanilla, and R. E. Taylor. 1985. Sodium channel activation in the squid giant axon. *J. Gen. Physiol.* 85:65–82.
- Zagotta, W. N., T. Hoshi, and R. W. Aldrich. 1991. Molecular separation of two inactivation processes in Shaker potassium channels (Abstract). *Biophys. J.* 59:3a.